

1-1-1979

Transformation of Atmospheric and Solar Illumination Conditions on the CCRS Image Analysis System

Francis J. Ahern

Philippe M. Teillet

David G. Goodenough

Follow this and additional works at: http://docs.lib.purdue.edu/lars_symp

Ahern, Francis J.; Teillet, Philippe M.; and Goodenough, David G., "Transformation of Atmospheric and Solar Illumination Conditions on the CCRS Image Analysis System" (1979). *LARS Symposia*. Paper 242.
http://docs.lib.purdue.edu/lars_symp/242

This document has been made available through Purdue e-Pubs, a service of the Purdue University Libraries. Please contact epubs@purdue.edu for additional information.

Reprinted from

**Symposium on
Machine Processing of
Remotely Sensed Data**

June 27 - 29, 1979

The Laboratory for Applications of
Remote Sensing

Purdue University
West Lafayette
Indiana 47907 USA

IEEE Catalog No.
79CH1430-8 MPRSD

Copyright © 1979 IEEE
The Institute of Electrical and Electronics Engineers, Inc.

Copyright © 2004 IEEE. This material is provided with permission of the IEEE. Such permission of the IEEE does not in any way imply IEEE endorsement of any of the products or services of the Purdue Research Foundation/University. Internal or personal use of this material is permitted. However, permission to reprint/republish this material for advertising or promotional purposes or for creating new collective works for resale or redistribution must be obtained from the IEEE by writing to pubs-permissions@ieee.org.

By choosing to view this document, you agree to all provisions of the copyright laws protecting it.

TRANSFORMATION OF ATMOSPHERIC AND SOLAR ILLUMINATION CONDITIONS ON THE CCRS IMAGE ANALYSIS SYSTEM

FRANCIS J. AHERN, PHILIPPE M. TEILLET
AND DAVID G. GOODENOUGH

Canada Centre for Remote Sensing

ABSTRACT

A software package for the transformation of atmospheric and illumination conditions (TASIC) has been implemented on the Canada Centre for Remote Sensing's Image Analysis System. This package offers three different transformations: (1) transformation to reflectance units; (2) transformation of illumination conditions; and (3) transformation to radiance units under standard atmospheric and illumination conditions.

Atmospheric parameters can be derived from four different sources, allowing users considerable flexibility. In particular, the method of obtaining atmospheric information from the LANDSAT signals from clear water bodies (Ahern et al. 1977 a, b) has been incorporated as one of the options. It offers high accuracy without the requirement of additional information derived from ground observations.

The TASIC procedure, including the acquisition of two-dimensional atmospheric information, is described in detail. Examples are given demonstrating the removal of atmospheric and solar illumination variations in a sequence of six LANDSAT images of the same area obtained between May and September 1976.

Systematic errors introduced by the uncertainty in the absolute calibration of the LANDSAT multispectral scanner are the most significant errors. The radiative transfer model used in the TASIC software also introduces significant systematic errors. Random errors are less important in the present procedures.

It is estimated that 60 to 90 percent of the variations due to atmospheric and illumination changes can be removed using the TASIC algorithm.

INTRODUCTION

In order for remote sensing measurements to have the greatest possible utility, the influence of factors unrelated to the targets of interest must be removed. This greatly facilitates multi-date and multi-sensor inter-comparisons and the interpretation of the remote sensing data in terms of intrinsic properties of the targets of interest. In the reflective part of the electromagnetic spectrum, the intrinsic property of

interest is reflectance, while the most important complicating effects are those due to variations in solar illumination and to atmospheric transmission and path radiance. Transformations taking these solar and atmospheric effects into account can be applied to measured radiances in order to obtain reflectance values or radiances under specified atmospheric and illumination conditions. Three such transformations have been implemented in a software package now available on the Canada Centre for Remote Sensing's Image Analysis System, which is built around a modified General Electric IMAGE 100 (Goodenough 1977, 1978).

II. APPROACHES TO ATMOSPHERIC AND ILLUMINATION CORRECTIONS

A. TYPES OF OUTPUT IMAGE DATA

1. Transformation to Reflectance Units.

In the case of a multispectral imaging sensor such as the LANDSAT multi-spectral scanner, the measured quantity is the radiance L in each spectral band for each of the many pixels in the scene. The desired intrinsic property is usually the hemispherical reflectance ρ . For a perfectly diffusing reflector viewed through the atmosphere, the reflectance is

$$\rho = \frac{\pi(L - L_p)}{HT}, \quad (1)$$

where H is the total downwelling irradiance, T is the atmospheric transmission, and L_p is the atmospheric path radiance.

The most desirable output from a transformation of atmospheric and solar illumination conditions (TASIC) would be an image calibrated in reflectance units. This would relieve the user of any further worry about atmospheric and illumination effects in the scene of interest. The TASIC procedure at CCRS can provide this form of output when the user is confident that the necessary accuracy is achievable with the data available. This usually implies using a relatively clear scene with several clear water bodies within a few kilometres of the study area, or independently acquired atmospheric transmission data for the time of satellite overpass.

2. Transformation of Illumination Conditions.

If detailed atmospheric information is not available, the radiances of a scene can still be transformed to those which would be observed under different illumination conditions. This transformation is of the form

$$L_n = \frac{H_n}{H} (L - L_p) + L_{pn}, \quad (2)$$

where the subscript n refers to the new illumination conditions.

3. Transformation of Scene Radiances Under Standard Conditions.

For some applications, the researcher may want a scene corrected to radiances which would be measured under conditions of standard illumination and atmospheric conditions rather than correcting to reflectances. The equation for such a correction is

$$L_s = \frac{H_s T_s}{HT} (L - L_p) + L_{ps}, \quad (3)$$

where the subscript s refers to standard conditions. This option is also available at CCRS through the TASIC software package. For good results, this approach requires the same high quality atmospheric information needed to correct to a reflectance image. In fact, the transformation given by equations (1) and (3) are linearly related through the constant parameters H_s , T_s and L_{ps} .

B. IDENTIFICATION AND DETERMINATION OF REQUIRED INPUT PARAMETERS

1. Bright/Dark Reflectors.

The most straightforward method of converting radiance measurements to reflectance values results from the fact that equation (1) is linear. If a scene contains one or more relatively dark objects of known reflectance and one or more relatively bright objects of known reflectance, these can be used to establish the linear relationship between radiances and reflectances. The rest of the scene can then be converted using the resulting linear equation. This method, fully demonstrated by Stanz (1978), has not yet been widely applied because the reflectance properties of natural targets are not sufficiently well understood to allow specification of known bright and dark calibration objects in the majority of LANDSAT (or airborne MSS) scenes.

Since atmospheric and illumination problems cannot generally be circumvented with calibration reflectors, they must be addressed at a more fundamental level. Therefore, each of the factors in equation (1) must be considered and evaluated by some means.

2. Total Downwelling Irradiance.

The total downwelling irradiance H (also known as the scene illumination) consists of a direct component contributed by light coming directly from the sun to the target, and a diffuse component contributed by light from the sky. The direct component is a function of the earth-sun distance, the solar zenith angle, and the atmospheric transmission. The earth-sun distance and solar zenith angle can be determined from the time of data acquisition.

Since attenuation of the direct component is primarily due to scattering by molecules and aerosols with single-particle albedos near unity, most of the radiation removed from the direct component of downwelling irradiance becomes part of the diffuse component. To a very good approximation, the total downwelling irradiance is independent of atmospheric transmission even though the direct and diffuse components are sensitive to changes in atmospheric transmission. Band 7 of the LANDSAT MSS is an exception because water vapour absorption is an additional source of direct beam attenuation in that bandpass. This effect has not been taken into account in the present atmospheric correction procedures, but there is no evidence that its omission gives rise to adverse results.

In short, the total downwelling irradiance can be computed to high accuracy from a knowledge of the time of data acquisition and the resulting illumination and viewing geometry. This allows illumination corrections to be made independently of detailed knowledge of the clarity of the atmosphere through which the observations were made.

For a complete conversion to reflectance, another multiplicative factor correcting for atmospheric transmission and an additive term correcting for path radiance must also be known.

3. Atmospheric Transmission from Ground Measurements.

The atmospheric transmission can be measured from the ground by observing the sun as a standard source of irradiance in a technique known as the Langley method (well explained by Rogers and Peacock 1973). Deepak and Box (1978 a, b) have recently shown how to correct these observations for the significant diffuse component included in the field of view of the measuring instrument if there is some knowledge of the scattering particle albedo and size distribution.

4. Path Radiance.

(a) Ground Measurement:

Rogers and Peacock (1973) have demonstrated that a technique originally suggested by Gordon (1973) can be used to infer path radiance from ground-based observations of sky radiance. This method gives results which agree well with those of accurate model atmosphere calculations (Miller and O'Neill 1977). How-

ever, the method requires the sun to be less than 45° above the horizon, with the consequence that observations to determine path radiance must often be separated in time from the actual satellite observations.

(b) Atmospheric Modelling:

Alternatively, it is possible to use a variety of atmospheric models to calculate the path radiance once the atmospheric transmission, the illumination and viewing geometry, and the mean background albedo are known. Unfortunately, in choosing an atmospheric model, a compromise must be made between speed and accuracy. This has partially been overcome at CCRS by the creation of a hybrid between the popular Turner model (Turner and Spencer, 1972) and a discrete ordinate calculation (O'Neill and Miller 1977, O'Neill et al 1978). In the latter work, the discrete ordinate method was found to give good absolute agreement between calculated and observed values of zenith sky radiance and nadir path radiance. The hybrid model computes the ratio of path radiance interpolated from the tables of O'Neill et al (1978) to Turner path radiance calculated for the same conditions. This ratio is then used to correct Turner model calculations for other viewing angles.

For input to the model atmosphere calculation, the illumination and viewing geometry can be computed from the time and location of data acquisition, and the atmospheric transmission is provided by ground observations through the Langley method. The average background albedo has second-order influence on the path radiance. Hence, typical or measured values for a given area and date can be used, or satellite data converted to reflectances with a standard atmosphere can be used. All three approaches are available with the TASIC algorithms.

5. Clear Water Bodies.

Ground-based measurements of specific parameters such as atmospheric transmission are acceptable for research projects where the necessary manpower and instrumentation can be made available. For operational applications of remotely sensed data, it is preferable to extract the necessary information from the satellite data themselves whenever possible. Previous work has shown that it is possible to extract both path radiance and transmission information from LANDSAT data if clear water bodies are present in the scene (Ahern et al 1977 a, b).

The technique has been implemented in the TASIC software package, enabling users to correct all or part of a LANDSAT scene containing clear water pixels. More specifically, measurements of path radiance over clear water pixels in the scene are fitted by a two-dimensional polynomial of order ≤ 2 . Then, inversion of the hybrid atmospheric model discussed in the previous section yields atmospheric transmittance.

III. OPERATION OF THE TASIC SOFTWARE

The most involved procedure in the software package is the use of clear water bodies for the

determination of atmospheric parameters. The more straightforward procedures involving the input of independent atmospheric data or the transformation to other solar illumination conditions are described in section E.

The conversion to reflectance units by the use of atmospheric information derived from clear water bodies can be divided into five logical stages, each of which requires a few minutes on the CCRS Image Analysis System (CIAS). Most stages require some judgement by the user or operator, so the procedure has been designed for easy interaction. The five stages are:

- (a) loading the appropriate portion of the LANDSAT scene of interest from disk or tape into the CIAS memory;
- (b) setting thresholds to isolate clear water bodies;
- (c) determination of the average path radiance over water bodies;
- (d) fitting of a two-dimensional function to path radiance over the scene;
- (e) creation of a two-dimensional radiometric correction function from path radiance and solar illumination information, followed by transformation of the scene (digital) values with that function.

Each of these steps will be discussed in more detail.

A. SCENE LOADING

The CIAS has a five-channel, 512 by 512 8-bit per pixel memory with which very rapid image processing can be accomplished. Three channels plus themes can be monitored simultaneously on a colour CRT display. All or part of a LANDSAT scene can be loaded into the memory from disk or tape. If an area larger than 512 by 512 pixels is loaded, lines and pixels are decimated by sufficient amounts to be accommodated by the memory.

The clear water bodies method of atmospheric parameter estimation will work best if the area of interest is surrounded by clear water bodies. The user should try to achieve this even if a larger area must be loaded with line and pixel decimation. Once the atmospheric parameters have been obtained, the central area can be re-loaded and then transformed at a larger scale.

B. ISOLATION OF CLEAR WATER BODIES

It is well known that LANDSAT band 7 can be used to distinguish water covered areas from dry land because of the strong infrared absorption of water. There exists a radiance level in this band below which only water pixels are recorded. However, the exact level of this threshold varies from scene to scene because of variations in atmospheric path radiance. Thus, it was decided that the task should be performed interactively for greater reliability.

On the CIAS, the threshold in a given band is varied with a graphics terminal by truncating the displayed histogram for that band. Pixels within the histogram limits are "alarmed" in bright green on the display screen and the change upon truncation is seen

instantaneously. Thus, the proper threshold to exclude land and mixed land/water pixels in band 7 can be quickly established. Cloud shadows over land are usually excluded by this procedure since they are generally brighter than water.

A similar procedure is employed to discriminate clear from turbid water with band 4. Of course, the experimenter should have sufficient knowledge of the study area to have confidence that there are clear as opposed to turbid water bodies in the vicinity.

Figure 1 shows the locus of the radiances of clear water bodies in the band 7-band 4 plane under a wide range of atmospheric conditions. Water bodies chosen above the dashed line are not clear enough to give good results. A lower limit has also been established. One point in Figure 1 lies below the lower limit. This point was obtained on a day (Sept. 12, 1976) when thin cirrus clouds were present over the water bodies in question. The techniques presented here are not expected to correct cirrus cloud obscuration properly since the ice crystals in them have very different optical properties than the liquid water aerosols which cause most of the aerosol backscatter on clear days.

If the atmospheric fitting program detects significant water areas above or below the limits in Figure 1, a warning message is displayed to the user. These limits may be modified in future as more data are acquired.

Thresholds are also set for bands 5 and 6 in order to exclude any drop-out pixels which may be present. The clear water pixels are then loaded onto a theme (a one-bit overlay) for subsequent use by the atmospheric fitting program.

C. DETERMINATION OF PATH RADIANCE OVER WATER BODIES

An interactive program which takes advantage of the special processing hardware of the CIAS is used to determine the path radiance over water bodies and fit a two-dimensional function to the path radiance across the scene. The investigator designates the area of interest with a rectangular cursor driven by a joystick. The CIAS is then used to determine the average intensity in this area. This information is necessary to estimate the average scene albedo, an input parameter for the model atmosphere calculations. Next, the investigator is asked to specify the number of subscenes (from 1 by 2 to 8 by 8) into which the scene is to be divided in horizontal and vertical dimensions. A small number of subscenes is sufficient if the atmosphere is relatively uniform across the scene, while a large number is necessary if the atmosphere varies significantly across the scene.

The program then determines the mean intensity, the standard deviation, and the geometric centroid coordinates of the water pixels in each subscene. This information is stored in a temporary disk file for subsequent processing.

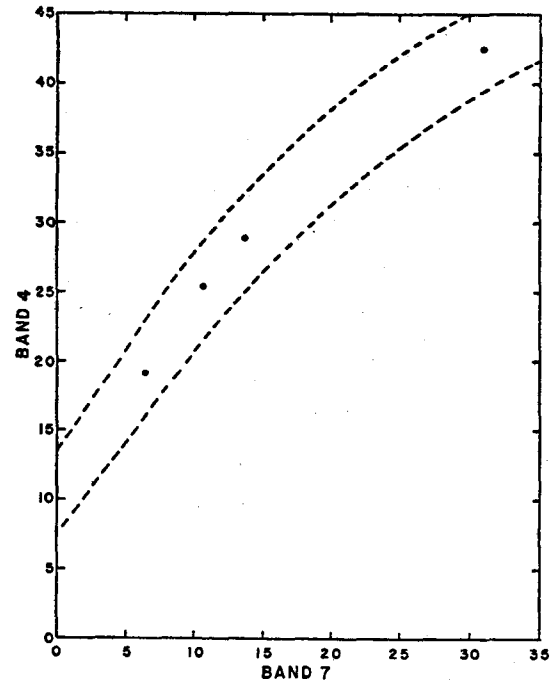


Figure 1: Water Pixel Loci. The five points plotted show the average value of clear water intensities on an 8-bit scale for five dates in 1976. The variation is caused by atmospheric and illumination changes from one date to the next. The upper dashed line separates relatively clear water from water too turbid to provide good atmospheric data. The point below the lower dashed line was obtained on a day when thin cirrus clouds were present. Such clouds have a different reflectance spectrum than liquid water haze and are not as well modelled in the atmospheric transformation.

D. TWO-DIMENSIONAL FITTING OF PATH RADIANCES

The mean water pixel intensities, standard deviations, and geometric centroids are read from the temporary disk file. The radiance contributed by the volume and surface reflectance of the water is estimated with reflectance values determined by Ahern et al (1977a). This value is subtracted from the mean intensities, leaving the contribution from atmospheric path radiance. The user then chooses between a constant, linear, or quadratic fit to the two-dimensional distribution of path radiance as a function of centroid coordinates. After this fit is performed, the residuals are displayed graphically for each channel in turn, together with the root mean square residual of all subscenes containing water pixels.

The errors to be expected with this function are also predicted and displayed over the whole scene of interest. This is particularly helpful in demonstrating how well a function established in an area containing

water bodies will extrapolate to an area with no clear water bodies.

Figure 2 shows an example of the plot of residual vectors with a constant (level plane) fit for band 6 of a scene from LANDSAT frame 210491-15055. Figure 3 plots the residuals for the same scene with a quadratic fit, illustrating the decrease in the individual and rms residuals. The predicted errors for the entire scene in the case of a quadratic fit are shown in Figure 4.

If available clear water bodies are limited to a small portion of the scene, care must be taken when extrapolating the fitted function to another part of the scene. Figure 5 plots the residuals with a quadratic fit to the water bodies in one corner of the same scene. Figure 6 shows the errors predicted across the whole scene on the basis of the quadratic fit. Note the rapid increase in the errors away from the corner in which the fit was actually done. The constant fit would be more reliable in this case (cf. Figure 7).

In view of the importance of choosing the optimum fitting function, the user can cycle through the procedure and display residuals and predicted errors until a satisfactory choice is made. Subsequently, the various scene and atmospheric parameters, together with the coefficients of the two-dimensional fitting function, are stored in a disk file for later use by the program which actually implements solar and atmospheric transformations.

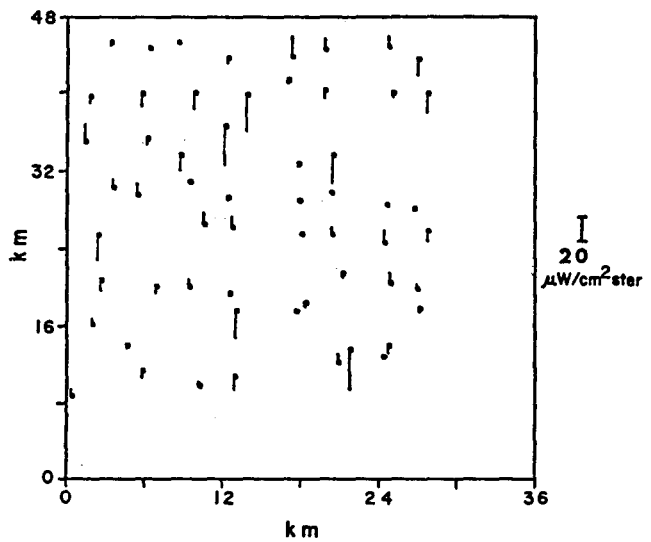


Figure 3: Vector Plot of Residuals, Quadratic Fit. The vectors show the difference between the measured path radiance and the path radiance removed by a two-dimensional quadratic function. The rms residual is $0.006 \text{ mw/cm}^2\text{sr}$.

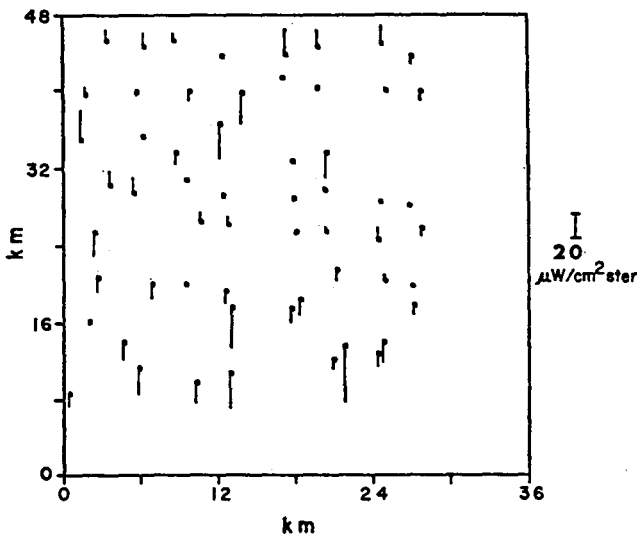


Figure 2: Vector Plot of Residuals, Constant Fit. The vectors show the difference between the measured path radiance and the path radiance removed by a two-dimensional constant function fitted to the eight by eight grid of points shown here. The rms residual is $0.008 \text{ mw/cm}^2\text{sr}$.

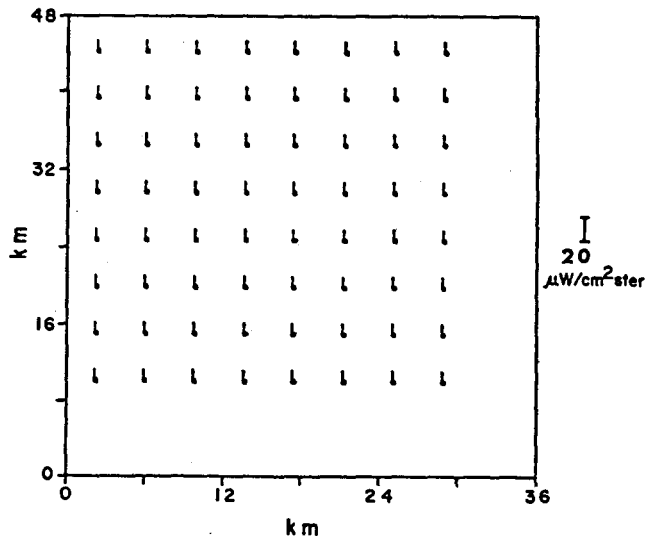


Figure 4: Vector Plot of Predicted Errors. This figure shows the predicted errors in the path radiance removed from a portion of scene 20491-15055 if the fit in Figure 3 were to be used.

E. SCENE TRANSFORMATION

The actual scene transformation is carried out in a separate program, thus facilitating solar illumination transformations and the use of sources of atmospheric parameters other than the clear water method. Four options are available for the source of parameters for use in the atmospheric correction:

- (a) an atmospheric parameter file generated as described in steps A to D;
- (b) atmospheric transmission values supplied by the researcher and average background reflectances determined from the scene data;
- (c) atmospheric transmission values and average reflectances supplied by the researcher;
- (d) default values for a standard atmosphere.

For options (c) and (d), steps A to D can be omitted.

Three output options are provided, corresponding to equations (1), (2), and (3). Conversion to reflectances (1) is recommended when the investigator has reliable atmospheric information. The illumination correction in option (2) can be used with or without additional atmospheric information. (A standard atmosphere is the default.) The transformation to radiances under standard conditions (3) is available for specialized research purposes but is not recommended for general use.

In the second option, the modified Turner model is invoked to compute values of irradiance and path radiance in equation (2) for the old and new illumination conditions. Any one of the four sources of atmospheric

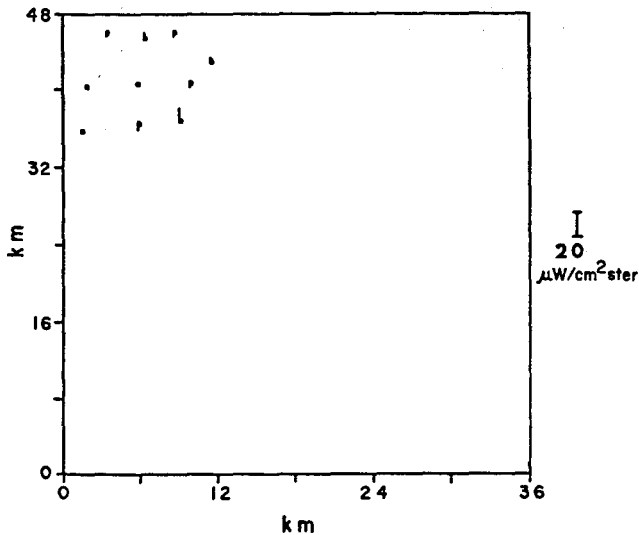


Figure 5: Vector Plot of Residuals, Corner of Scene 20491-15055. These are the residuals from a quadratic fit to the points in the corner of the scene. The rms residual is $0.007 \text{ mw}/\text{cm}^2 \text{ sr}$.

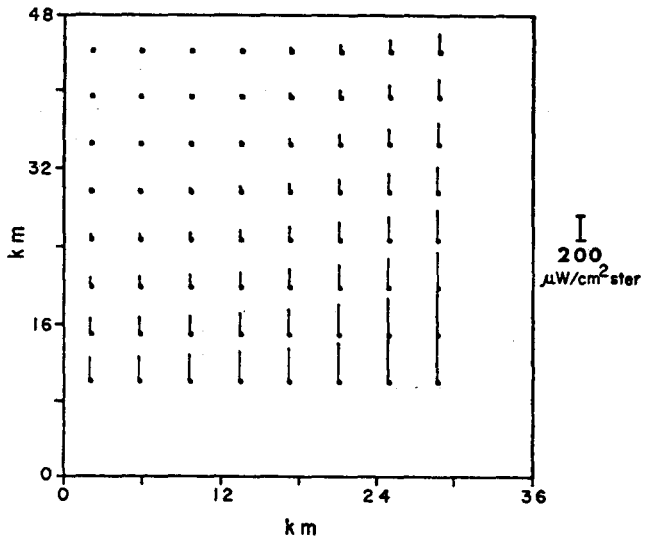


Figure 6: Predicted Errors from Quadratic Fit to Corner Data. This figure illustrates how the predicted errors become very large when a quadratic fit is extrapolated to areas far from the region where the fitted data were obtained.

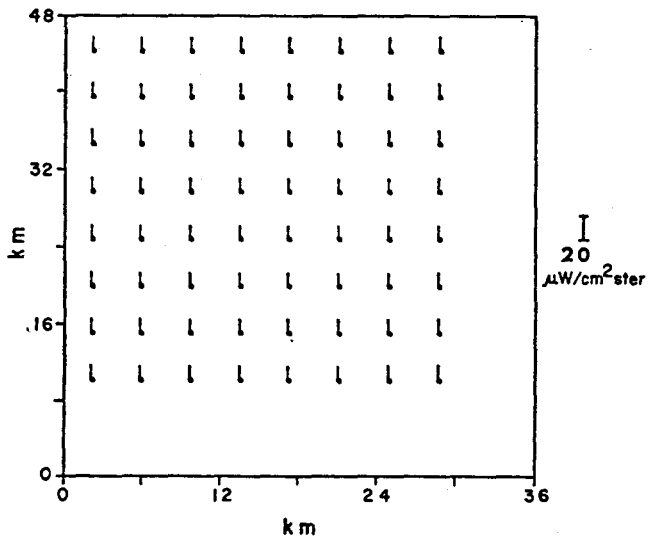


Figure 7: Predicted Errors from Constant Fit to Corner Data. A constant fit cannot "blow up" away from the fitted points the way a quadratic fit can. However, the experimenter should have some confidence in the uniformity of atmospheric conditions for the scene being transformed if an extrapolation like this is to be reliable.

parameters described above may be used. Care is taken to separate the effects of illumination conditions on the direct and diffuse components of irradiance. Although it is a relatively minor effect, earth curvature is also taken into consideration since the solar zenith angle varies from point to point. Thus, while it must still assume Lambertian reflectance, the present approach to solar illumination transformations is implemented in a more realistic fashion and should produce better results than a simple cosine correction.

The new solar elevation angle can be specified in one of four ways:

- (a) standard 50 degrees (default);
- (b) solar elevation at frame centre;
- (c) highest solar elevation occurring at frame centre latitude (summer solstice);
- (d) user specified.

The earth curvature correction correction is carried out in all cases.

If the user has chosen to convert to reflectances or to radiances for standard conditions, new solar elevation angles need not be specified by the user and the interaction just described does not occur. However, the computer program proceeds as in case (b) for the former and case (a) for the latter conversion schemes.

Equations (1), (2), and (3) can all be written as linear transformations of the form

$$S' = A(x,y) S + B(x,y) \quad , \quad (4)$$

where S and S' represent the original and transformed LANDSAT digital values, respectively. $A(x,y)$ and $B(x,y)$ are functions of solar, atmospheric, and geometric quantities at a given point (x,y) . A and B values are computed in each band for a grid of points in the frame to be transformed and subsequently fitted by two-dimensional quadratic functions. LANDSAT digital levels in each band can then be transformed at all points or in a user-specified portion of the scene.

IV. VERIFICATION OF THE REFLECTANCE TRANSFORMATION

A. REFLECTANCE COMPARISON

The most satisfactory verification of the TASIC methodology would be to compare LANDSAT data transformed to reflectance units with simultaneously acquired ground or aircraft data well calibrated in reflectance units. Such a comparison was attempted using airborne data acquired with the Miller-Pieau Photometer (MPPH) as part of a previous investigation (Ahern et al 1977a). LANDSAT and aircraft reflectances over water bodies are in good agreement. However, this serves only to verify that the

computations are numerically correct since the same aircraft data set was used to establish the path radiance correction in the present method. A more significant comparison of aircraft and LANDSAT data over land areas was not possible because of the significantly different fields of view of the two sensors and the difficulty of determining the exact pointing direction of the aircraft sensor. Since the MPPH is a profiling sensor, averaging pixels will not overcome these problems entirely unless extended uniform targets are used for the comparison. Such land targets were not included in the investigation by Ahern et al. (1977a) since that experiment was carried out for different purposes. Thus, there remains a need for a data set specifically suited to a reflectance comparison with due consideration given to the types of sensors involved.

B. TIME VARIABILITY OF TARGETS IN A SCENE

A less conclusive but still interesting verification is to study the time variability of the reflectances of several different targets in a scene. Table 2 lists six targets chosen for this purpose. Figures 8 and 10 show the original radiances in LANDSAT bands 4 and 6, respectively, for each target on six dates in the summer of 1976. Figures 9 and 11 show the corresponding reflectances computed for LANDSAT bands 4 and 6. The following points can be made concerning the transformed data.

- (a) Grand Lake remained essentially constant all summer.
- (b) McLeod Lake underwent changes in radiance normally associated with a cycle of biological activity. This is consistent with the fact that the lake has no outlet and lies downstream from a small town.
- (c) Band 4 values for the forest area exhibited a decrease at the beginning and an increase at the end of the growing season. This behaviour is characteristic of increasing chlorophyll absorption during the course of the growing season.
- (d) Although booms were moved and/or logs were added or removed, the log booms remained approximately constant.
- (e) Both the quarry and the gravel pit had considerable brightness variations from pixel to pixel, making it difficult to estimate meaningful averages. Correlated changes manifested themselves in the values for these targets. Since the deepest dip was on September 12, 1976 when cirrus clouds were present (see Section III.B), this might be a residual atmospheric effect. However, the log boom and forest reflectances do not show correlated changes.

This exercise demonstrates how TASIC decreases the masking of intrinsic variations which is caused by changing atmospheric and illumination conditions, even though it does not prove that the changing conditions are completely corrected.

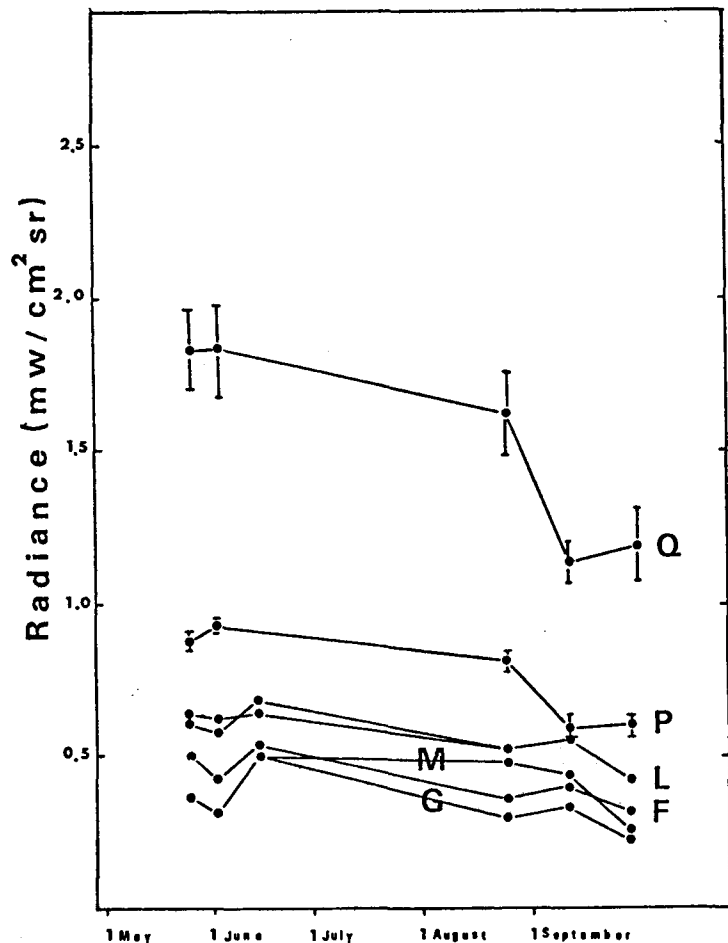


Figure 8: Radiance, Band 4. The raw band 4 radiances on six dates in 1976 are shown for six targets: Q: Quarry; P: Gravel Pits; L: Log Booms (2); M: McLeod Lake; F: Forest; G: Grand Lake. The error bars show the standard deviation of the radiances of pixels averaged for each point.

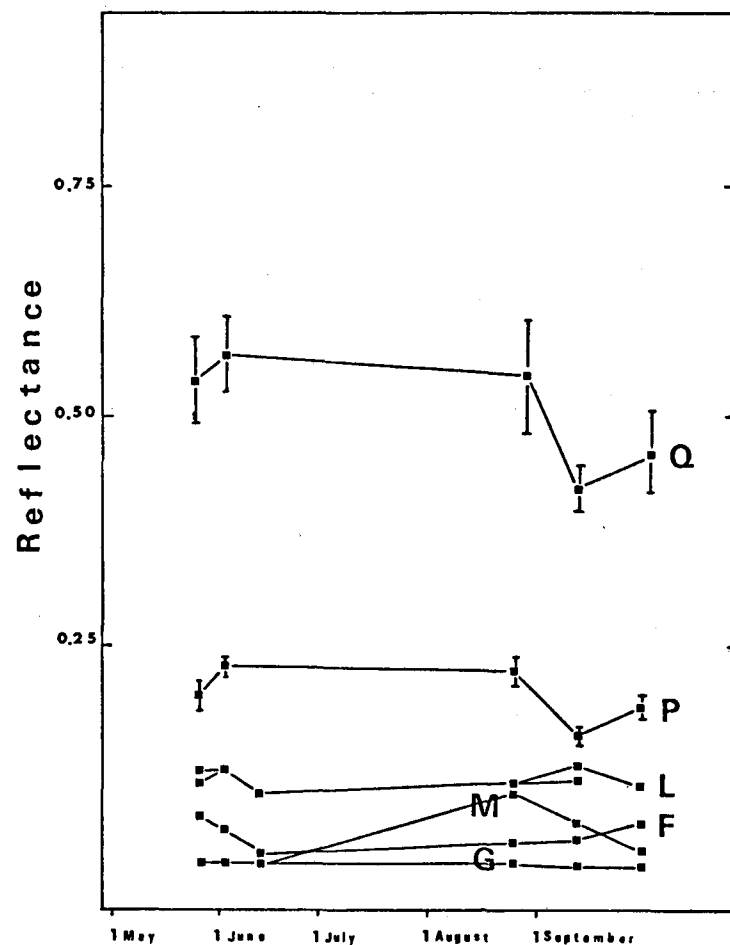


Figure 9: Reflectance, Band 4. These reflectances have been obtained by applying the TASIC procedure to the six scenes listed in Table 2, using the clear water body method of atmospheric parameter estimation. Grand Lake is typical of the clear water bodies used for this technique and its variations have been removed. Some of the variations of McLeod Lake have been removed, leaving those typical of a summer cycle of biological activity. The forest area shows decreased reflectance during the growing season, as expected from chlorophyll absorption. The variations in the quarry and gravel pit reflectances are unexplained.

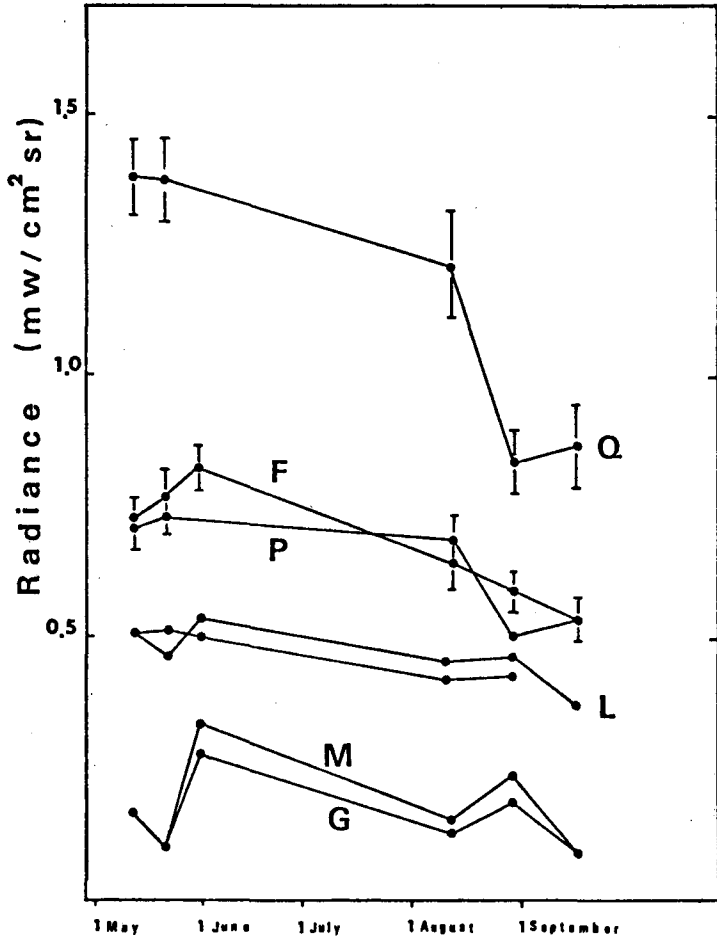


Figure 10: Radiance, Band 6. The untransformed radiances in band 6 for the same six targets described in Figure 8 are shown here.

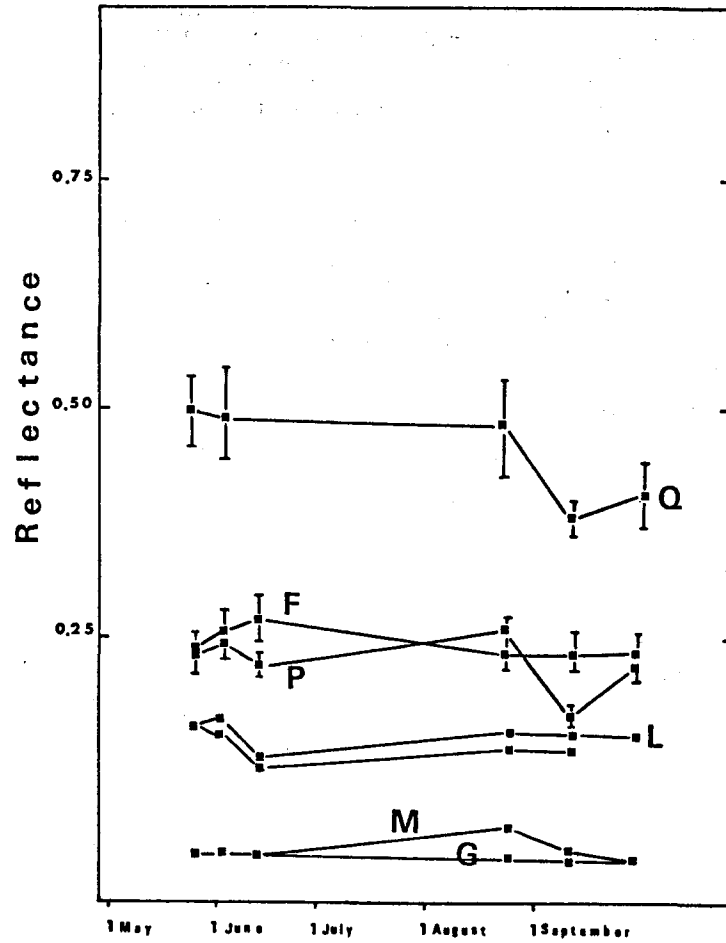


Figure 11: Reflectances, Band 6. As in band 4, the TASIC procedure has removed much of the variability of the six targets, especially the water bodies.

C. COMPARISON OF EXTINCTION COEFFICIENTS

Of the two multiplicative factors in equations (1), (2), and (3), the atmospheric transmission T is more subject to systematic errors. The transmission is estimated by an indirect method involving an absolute path radiance measurement and a model atmosphere calculation, both of which may have significant systematic errors. To estimate the magnitude of these errors, the atmosphere discussed in Section B.5 was compared with the extinction coefficient measured near McGregor Lake at the time of satellite overpass. This comparison is shown graphically in Figures 12-15. Significant systematic differences are present and these vary from band to band. In addition to the problems with the estimated extinction coefficients, the measured extinction coefficients may be up to 20 percent low (Deepak and Box 1978 a, b). This is reflected in the error bars shown in Figures 12-15.

The results of a regression analysis for these data are presented in Table 3. Although systematic differences between observed and calculated extinction coefficients remain, they are smaller than those obtained previously (Table XIII, Ahern et al. 1977a) with the unmodified Turner model (Turner and Spencer 1972).

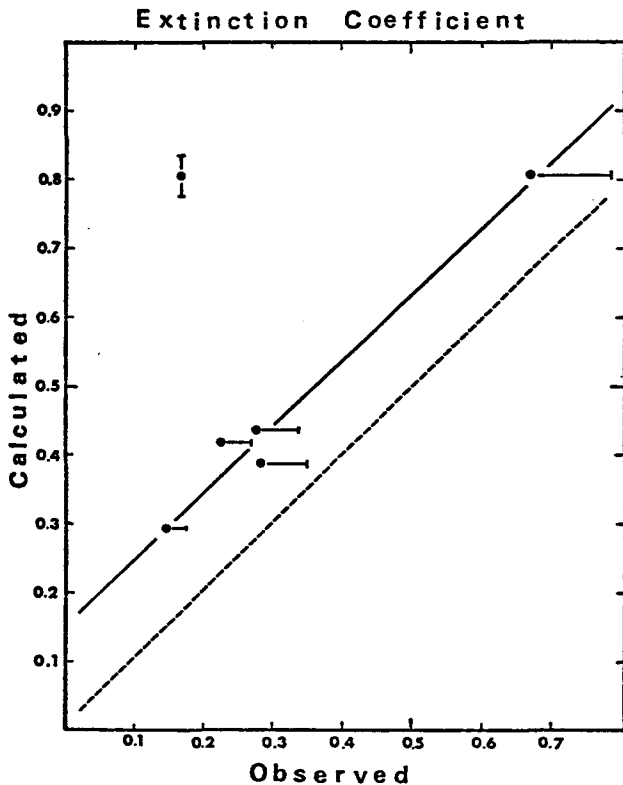


Figure 12: Extinction Coefficient, Band 4.

These figures show the extinction coefficients calculated from an inversion of the atmospheric model plotted against extinction coefficients measured from the ground at the time of satellite overpass. The vertical error bar shows the error introduced by the expected error in the estimation of path radiance. The horizontal error bar indicates the possibility of an extinction coefficient being underestimated by about 20% because of light from the solar aureole in the measuring field of view, as suggested by Deepak and Box (1978 a, b).

Further progress will require consideration of the accuracy of the absolute radiance calibration of the LANDSAT multispectral scanner, as well as improved methods of measuring atmospheric extinction and better atmospheric models.

V. ERROR ANALYSIS

A transformation such as TASIC involving the use of imperfectly known quantities introduces random and systematic errors. It is very important to understand the sources and effects of these errors as they relate to the desired use of the data in order to determine which transformation, if any, should be employed.

A. RANDOM ERRORS

Random errors and their propagation have been discussed extensively in previous publications (Ahern et al. 1977a, b). The discussion will not be repeated here except to mention that no evidence of sun glint on water bodies smaller than a few kilometres in size has been found at Canadian latitudes. Thus, there is a reasonable degree of confidence that sun glint is not a significant source of error.

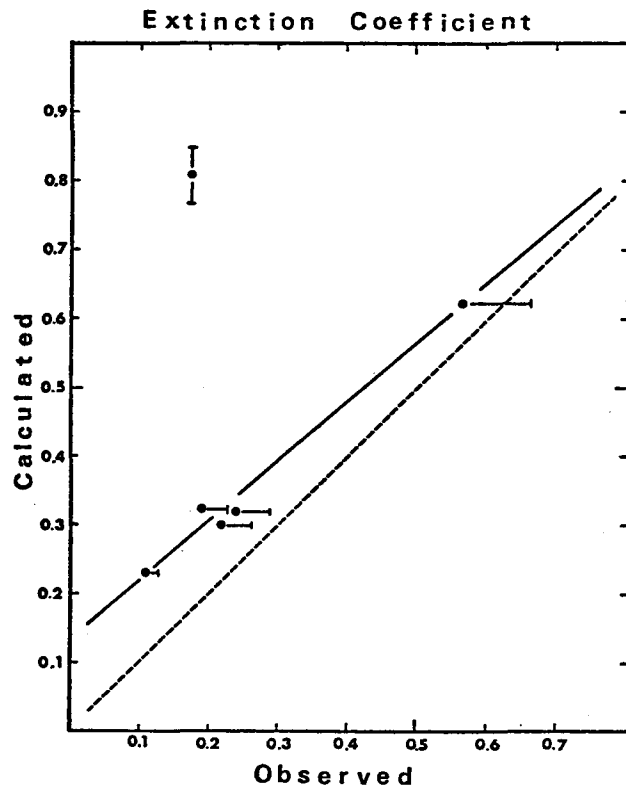


Figure 13: Extinction Coefficient, Band 5.

Table 4 gives the expected random errors introduced by the clear water method of atmospheric parameter estimation at the two extremes of the radiance scale, $L = L_0$ and $L = L_{max}$, in both radiometric units and CAL3 digital values*. The errors introduced into reflectance measurements by these random errors are also presented in Table 4.

B. SOURCES OF SYSTEMATIC ERRORS

The three primary sources of systematic errors affecting the TASIC results are as follows:

(a) Systematic errors are present in the LANDSAT MSS calibration. There is little in the literature concerning the absolute accuracy of the LANDSAT MSS calibration. One document supplied by the manufacturer of the LANDSAT-2 MSS suggests that its solar calibration values in orbit are within about 15% of those expected from prelaunch calibration (Lansing 1977). Therefore, a value of 0.15 may be chosen as representative of the systematic error in the absolute calibration of this instrument.

(b) Errors introduced in the hybrid model atmosphere used to calculate path radiance have been estimated by comparing path radiances derived from LANDSAT data with path radiances calculated for the conditions under which the LANDSAT data was acquired. This comparison is discussed by O'Neill et al. (1978). Because they are dependent on the absolute LANDSAT calibration, the magnitude of these systematic errors may themselves be in error.

(c) Errors introduced by the inversion of the hybrid model atmosphere to obtain transmission corrections have been estimated from the regression analysis outlined in Section IV.C and are presented in Table 3.

*The CAL3 calibration used at the Canada Centre for Remote Sensing was adopted for this study. This is a scale of 256 digital levels, where a digital value of 0 corresponds to $0.0 \text{ mw/cm}^2 \text{ sr}$ and a digital value of 255 corresponds to the L_{max} values given in Table 4. For more information, consult Ahern and Murphy (1979).

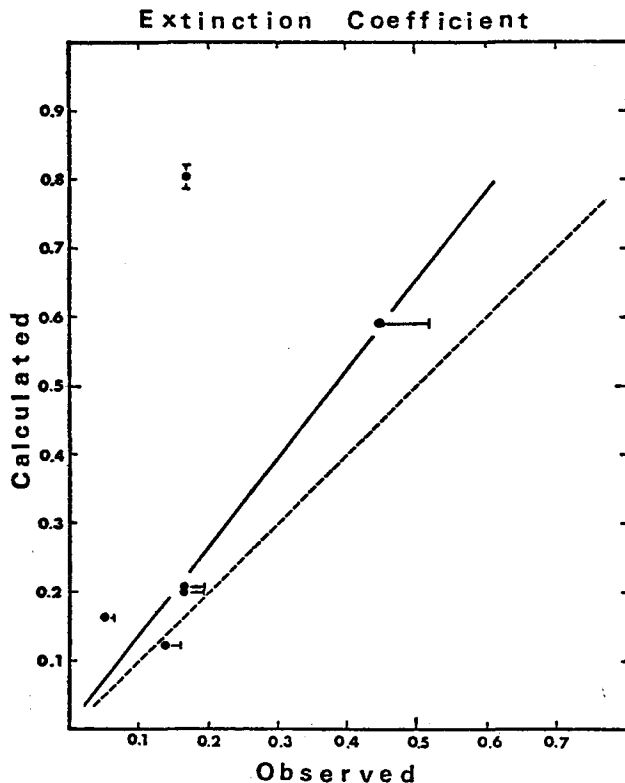


Figure 14: Extinction Coefficient, Band 6. The data for September 12, 1976 have not been used in FIGURES 12-15 since the presence of cirrus clouds makes the use of the existing radiative transfer model unreliable.

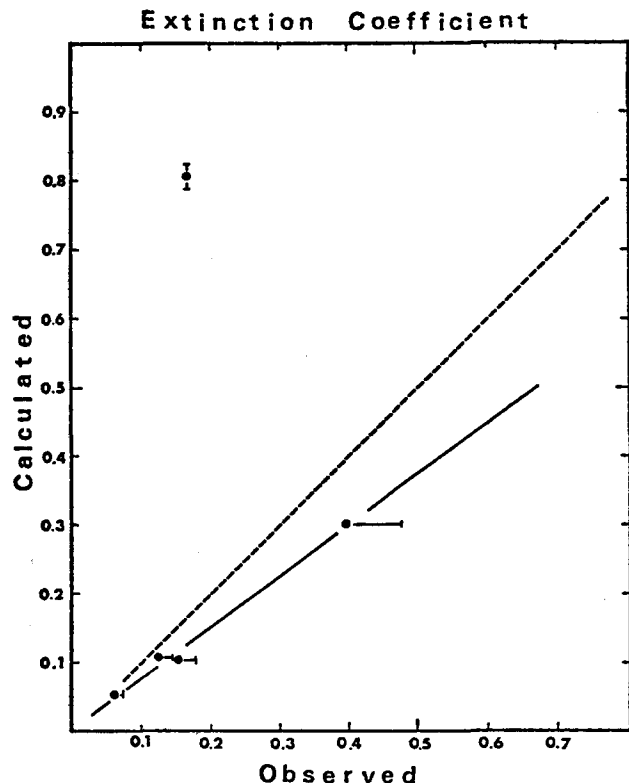


Figure 15: Extinction Coefficient, Band 7. The data for June 5, 1976 could not be used here since band 7 was not properly calibrated on LANDSAT-1

(d) The illumination transformation (Section A.2) is designed to be performed in the absence of accurate atmospheric data. Systematic errors may be introduced in the transformation of path radiance by the assumption of standard conditions when the actual ones are considerably different.

C. EFFECTS OF SYSTEMATIC ERRORS

1. In Transformation to Reflectances (Option 1).

The transformation to reflectances is accomplished through equation (1). Systematic errors introduced by this transformation are described by:

$$\Delta\rho = \frac{\pi}{HT} \left\{ \left[\frac{(L-L_p)}{T} \Delta_m(T) \right]^2 + \left[\Delta_c(L-L_p) \right]^2 \right\}^{1/2} \quad (5)$$

Table 5 describes the symbols in equation (5) and lists typical values used in subsequent analysis. The first term in equation (5) is the systematic error introduced in the transmission calculation, while the second is the systematic error introduced in the calibration of the LANDSAT MSS. As discussed in Section II.B.2, the error in computing the illumination is expected to be quite small and negligible compared to the two terms of equation (5).

Results of the calculations with equation (5) are presented in Table 6. A number of important insights can be gleaned from an inspection of this table.

(a) There is negligible systematic error in the reflectance from objects for which the measured radiance equals the path radiance. In other words, there is no additive or zero point error. This is a reflection of the confidence there is in the constancy and apparent darkness of the many clear lakes in the Canadian Shield. The random error (see Table 4) will be less than ± 0.01 times reflectance in all four bands.

(b) The fractional systematic error in reflectance $f(\rho)$ is too high to allow reliable comparison between LANDSAT derived reflectances and reflectances measured from the ground or the air. (For example, a 24 percent systematic error may be present in band 4 under standard conditions.) However, a single object in a scene whose reflectance is well known and relatively high can serve as a calibration target to remove most of this systematic effect. A differential measure of fractional systematic error, such as the systematic error which would remain between a hazy scene and a normal scene after both were transformed to reflectance, is considerably smaller. (This quantity is called $f_h(\rho) - f(\rho)$ in Table 6. Note that the differential error in band 4 is eight percent.) The TASIC procedure is therefore useful for intercomparison of scenes acquired under different conditions, as previously demonstrated in Section IV.B.

2. In Illumination Transformation (Option 2).

The illumination transformation is accomplished through equation (2). Systematic errors introduced by the transformation are estimated from:

$$\Delta L_n = \left\{ \left[\frac{H_n}{H} \Delta_c(L) \right]^2 + \left[\Delta_T(C) \right]^2 + \left[\Delta_m(C) \right]^2 \right\}^{1/2} \quad (6)$$

The first term of equation (6) relates to the error in the absolute calibration of the LANDSAT MSS. The second term represents the error introduced into the path radiance transformation by assuming standard atmospheric conditions when the actual conditions differ. The third term is an expression of the systematic error in the hybrid model atmosphere calculation of the change in path radiance between the original and the new solar elevation angles.

The symbols in equation (6) and typical values used in subsequent analysis are given in Table 7. These have been derived from two sample calculations of the change in path radiance resulting from a change of solar elevation angle from 25° to 50°. A standard atmosphere was used in one calculation while in the second, hazy conditions were assumed (see Table 5 for values).

The systematic error introduced by the model was estimated from the analysis of O'Neill et al. (1978). The results of calculations with equation (7) are shown in Table 8. At the low end of the radiance scale ($L = L_p$), the primary source of systematic errors is the uncertainty in the hybrid model atmosphere calculation of the change in path radiance caused by the change in solar zenith angle. At the middle of the radiance scale ($L = \frac{1}{2} L_{max}$), the primary source of error is the 15% uncertainty in the absolute calibration of the LANDSAT MSS. ($\frac{1}{2} L_{max}$ was used rather than L_{max} because it would not be realistic to discuss increasing the full scale brightness by a factor of 1.8.)

The absolute radiometric calibration error is not present when working in LANDSAT digital units. In this case, the additive error in the path radiance transformation is the only significant error, as can be seen from Table 8.

3. In the Radiance Transformation to Standard Conditions (Option 3).

The equation used for estimating systematic errors in the radiance transformation is:

$$\Delta L_s = \left\{ \left[\frac{H_s}{H} (L-L_p) \Delta_m \left(\frac{T_s}{T} \right) \right]^2 + \left[\frac{H_s T_s}{HT} \Delta_c(L-L_p) \right]^2 + \left[\Delta_m(L_{ps}) \right]^2 \right\}^{1/2} \quad (7)$$

A description of the symbols in equation (7) and typical values used in this analysis are given in Table 9. Results of the evaluation of equation (7) with the values in Table 9 are present in Table 10.

(a) Absolute Units

The major source of systematic errors at low radiances (line 1 of Table 10) is the error introduced by the model atmosphere calculation (third term of equation (7)). The major systematic errors at high radiances (line 2 of Table 10) are caused by the error in the absolute radiometric calibration of the LANDSAT MSS. As in the case of reflectance units, these systematic errors are too high to allow reliable comparison between LANDSAT measurements and measurements obtained from ground or airborne sensors. However, a single bright target measured both by LANDSAT and by a ground or airborne radiometer can serve to remove most of this error. It is important that a uniform area be chosen for this reference target to avoid problems arising from the differing fields of view of LANDSAT and the other sensors.

(b) Landsat Digital Units

When a LANDSAT digital calibration is used for intercomparison of two or more LANDSAT scenes, the errors of absolute calibration are eliminated, leaving those arising from the TASIC procedure itself. Table 10 gives the total systematic error for a single scene transformed to standard atmospheric and illumination conditions. The same table also shows the differential error between two scenes transformed to standard conditions (where one scene is acquired through a standard atmosphere and the other is acquired through a hazy atmosphere), as well as the error introduced by uncorrected atmospheric variations.

For low radiances, the error in a single scene (line 3) is smaller than the error expected from uncorrected atmospheric variations (line 5). The differential error (line 4) is zero because taking the difference between the two scenes removes the systematic error introduced in estimating the path radiance under standard conditions.

For high radiances, the systematic errors in the single scene transformation (line 6) and the two scene differential errors (line 7) are lower than those introduced by atmospheric changes (line 8). Hence this transformation can be valuable in removing much of the scene-to-scene variation caused by atmospheric changes.

It can be seen from Table 10 that a transformation to radiances under standard conditions gives rise to smaller multiplicative errors than the reflectance conversion, but that this is achieved at the cost of introducing an additive error in the estimate of standard path radiance. Researchers may prefer one transformation with its attendant errors over the other. However, it should be emphasized that the two transformations are really just different expressions of the same results. Reflectance data

can be converted to radiance units for standard conditions by simply applying a scale factor and an offset. As long as all data in a multi-date or multi-sensor comparison are placed on the same scale, subsequent analysis should not be affected by the choice of one correction scheme over the other.

IV. SUMMARY AND CONCLUSIONS

A transformation of atmospheric and solar illumination conditions (TASIC) software package has been implemented on the CCRS Image Analysis System. Three different transformations are available, each of which can employ one of four different sources of atmospheric information.

The transformation to reflectance units with atmospheric parameter input from clear water bodies has been demonstrated to remove most of the variability caused by changing atmospheric and illumination conditions.

An analysis of random and systematic errors has shown that present systematic effects result in larger errors than random effects. Of the two major sources of systematic errors, the uncertainty in the absolute calibration of the LANDSAT multispectral scanner generally introduces larger errors than those introduced by the imperfect radiative transfer model used for estimation and transformation of atmospheric conditions. Future progress will require more accurate absolute calibration of satellite sensors and the adoption of better atmospheric models.

Nevertheless, for an intercomparison of two or more LANDSAT MSS scenes, the absolute calibration error is avoided and the procedure described in this paper should reduce the errors caused by atmospheric variability by 80-90 per cent for low brightness portions of a scene and by 60-80 percent for high brightness portions of a scene.

REFERENCES

- Ahern, F.J. and Murphy, J. 1979, Radiometric Calibration and Correction of LANDSAT-1, -2, and -3 MSS Data, Canada Centre for Remote Sensing Research Report.
- Ahern, F.J., D.G. Goodenough, S.C. Jain, V.R. Rao and G. Rochon 1977a, Use of Clear Lakes as Standard Reflectors for Atmospheric Measurements, Proceedings of the Eleventh International Symposium on Remote Sensing of Environment, Environmental Research Institute of Michigan, pp. 731-755.
- Ahern, F.J., D.G. Goodenough, S.C. Jain, V.R. Rao and G. Rochon 1977b, LANDSAT Atmospheric Corrections at CCRS, Proceedings of the Fourth Canadian Symposium on Remote Sensing, Canadian Aeronautics and Space Institute, pp. 583-594.

Deepak, A. and M.A. Box 1978a, Forward Scattering Corrections for Optical Extinction Measurements in Aerosol Media. 1: Monodispersions, Appl. Opt., 17, pp. 1900-2908.

Deepak, A. and M.A. Box 1978b, Forward Scattering Corrections for Optical Extinction Measurements in Aerosol Media. 2: Polydispersions, Appl. Opt., 17, pp. 3169-3176.

Goodenough, D.G. 1977, The Canada Centre for Remote Sensing's Image Analysis System (CIAS), Proceedings of the Fourth Canadian Symposium on Remote Sensing, Canadian Aeronautics and Space Institute, pp. 227-244.

Goodenough, D.G. 1978, Programming Hardware for Remote Sensing Image Analysis, National Computer Conference, AFIPS Conference Proceedings, 47, 119-129.

Gordon, J.I., J.L. Harris Sr., and S.Q. Duntley 1973, Measuring Earth-to-Space Contract Transmittance from Ground Stations, App. Op. 12, 1317.

Lansing, J. 1977, private communication.

O'Neill, N.T. and J.R. Miller 1977, Comparison of Two Methods to Determine the Path Radiance Observed from Above the Atmosphere, Proceedings of Fourth Canadian Symposium on Remote Sensing, Canadian Aeronautics and Space Institute, pp. 573-582.

O'Neill, N.T., J.R. Miller and F.J. Ahern 1978, Radiative Transfer Calculations for Remote Sensing Applications, Proceedings of the Fifth Canadian Symposium on Remote Sensing, Canadian Aeronautics and Space Institute.

Rogers, R.H. and K. Peacock 1973, A Technique for Correcting ERTS Data for Solar and Atmospheric Effects, Symposium on Significant Results Obtained from the Earth Resources Technology Satellite-1, NASA SP-327, Vol. I, Section B, pp. 1115-1122.

Stänz, K. 1978, Atmosphärische Korrekturen von Multispektraldaten des Erderkundungssatelliten LANDSAT-2, Ph.D. Dissertation, University of Zurich.

Turner, R.E. and M.M. Spencer 1972, Atmospheric Model for Correction of Spacecraft Data, Proceedings of the Eighth International Symposium on Remote Sensing of Environment, Environmental Research Institute of Michigan, pp. 895-934.

Table 1
Standard Conditions for the Four LANDSAT MSS Bands

<u>Symbol</u>	<u>Description</u>	<u>Band 4</u>	<u>Band 5</u>	<u>Band 6</u>	<u>Band 7</u>
A_{sun}	Solar elevation angle	50°	50°	50°	50°
$\bar{\rho}$	Average background albedo	0.11	0.09	0.21	0.25
T_s	Atmospheric transmission	0.68	0.73	0.81	0.90
τ_s	Atmospheric extinction	0.386	0.315	0.211	0.105
L_{ps}	Path radiance ($\text{mw}/\text{cm}^2\text{sr}$)	0.286	0.164	0.153	0.185
H_s	Total irradiance (mw/cm^2)	12.196	10.815	9.226	18.903

Table 2
Targets and Dates of Time Variability Study

<u>Description</u>	<u>Latitude</u>	<u>Longitude</u>	<u># of Pixels Sampled</u>			
Grand Lake	45°42'N	75°39'W	36			
McLeod Lake	45°46'N	75°40'W	12			
Forest near Lac Ste Hélène	45°48'N	75°38'W	252			
Log Booms on Lac l'Escalier	45°50'N	75°39'W	20			
Gravel pit near Wilson's Corners	45°38'N	75°49'W	4			
Quarry near Wakefield	45°38'N	75°54'W	9			
Date(1976):	May 27	June 5	June 14	Aug. 25	Sept. 12	Sept. 30
Scene ID:	20491-15055	11413-14384	20509-15052	20581-15031	20599-15025	20617-15021

Table 3
Regression Analysis of Estimated (Ordinate) Versus Observed
(Abcissa) Extinction Coefficients

LANDSAT Band	No. of Points	Slope		Intercept		r^2
		Mean	Error	Mean	Error	
4	5	0.963	.082	.154	.030	.979
5	5	0.850	.063	.141	.019	.984
6	5	1.282	.194	.005	.046	.936
7	4	0.734	.048	.006	.011	.992
4-6	15	1.061	.086	.087	.026	.921
4-7	19	1.085	.115	.051	.033	.840

Table 4
Random Errors After Atmospheric Correction by the Clear
Water Method for the Four LANDSAT Bands

	Band 4	Band 5	Band 6	Band 7
Typical path radiance L_p ($\text{mw}/\text{cm}^2 \text{sr}$)	0.286	0.164	0.153	0.185
Random error at $L = L_p$ ($\text{mw}/\text{cm}^2 \text{sr}$)	0.012	0.016	0.007	0.016
CAL3 Units*	1	2	1	1
Reflectance Units†	0.005	0.006	0.003	0.003
Maximum CAL3* radiance, L_{max} ($\text{mw}/\text{cm}^2 \text{sr}$)	3.00	2.00	1.75	4.00
Random error at $L = L_{\text{max}}$ ($\text{mw}/\text{cm}^2 \text{sr}$)	0.071	0.071	0.027	0.063
CAL3 Units	6	9	4	4
Reflectance Units	0.027	0.028	0.011	0.012

* CAL3 is a 256 level calibrated digital scale for LANDSAT MSS data used at the Canada Centre for Remote Sensing. A digital level of 0 corresponds to $0.000 \text{ mw}/\text{cm}^2 \text{sr}$ while 255 corresponds to the values given above. For further discussion see Ahern and Murphy (1979).

† The radiance errors have been corrected to equivalent reflectance errors using equation (1) with standard values for H, T, and L_p taken from Table 1.

Table 5

Variables Used in the Reflectance Error Analysis for the Four LANDSAT Bands

<u>Symbol</u>	<u>Description</u>	<u>Band 4</u>	<u>Band 5</u>	<u>Band 6</u>	<u>Band 7</u>
$\Delta\rho$	Systematic error in reflectance	See Table 6			
T	Atmospheric transmission: Standard value Typical low value (hazy conditions)	0.68 0.57	0.73 0.62	0.81 0.71	0.90 0.79
$\Delta_m(T)$	Systematic error in T	0.13	0.10	0.07	0.04
L	LANDSAT measured radiance ($\text{mw}/\text{cm}^2\text{sr}$)				
L_{\max}	Max CAL3 radiance ($\text{mw}/\text{cm}^2\text{sr}$)	3.00	2.00	1.75	4.00
L_p	Path radiance ($\text{mw}/\text{cm}^2\text{sr}$): Standard Conditions Hazy conditions	0.286 0.360	0.164 0.217	0.153 0.224	0.185 0.356
H	Total irradiance on target (mw/cm^2): Standard conditions Hazy conditions	12.196 12.084	10.815 10.721	9.226 9.173	18.903 18.812
$\frac{\Delta_c(L)}{L}$	Systematic error in absolute calibration of LANDSAT MSS	0.15	0.15	0.15	0.15

Table 6

Systematic Errors in Reflectance Conversion for the Four LANDSAT Bands

<u>Symbol</u>	<u>Description</u>	<u>Band 4</u>	<u>Band 5</u>	<u>Band 6</u>	<u>Band 7</u>
ρ_{\max}	Reflectance corresponding to full scale CAL3 radiance under standard conditions	1.03	0.73	0.67	0.70
$\Delta\rho_s$ ($L=L_p$)	Systematic error in reflectance when $L = L_p$ (standard conditions)	0.0	0.0	0.0	0.0
$\Delta\rho_{\max}$ ($L=L_{\max}$)	Systematic error in reflectance when $L = L_{\max}$ (standard conditions)	0.25	0.15	0.12	0.11
$\frac{f_s(\rho)}{\Delta\rho_{\max}}$	Fractional systematic error in reflectance (standard conditions)	0.24	0.20	0.17	0.15
$f_h(\rho)$	Fractional systematic error in reflectance (hazy conditions)	0.32	0.25	0.20	0.17
$\frac{f_h(\rho)}{f_s(\rho)}$	Differential fractional systematic error.	0.08	0.05	0.03	0.02

Table 7

Variables Used in the Illumination Transformation for the Four LANDSAT Bands

<u>Symbol</u>	<u>Description</u>	<u>Band 4</u>	<u>Band 5</u>	<u>Band 6</u>	<u>Band 7</u>
ΔL_n	Systematic error in transformed radiance (mw/cm ² sr)	See Table 8			
L	LANDSAT measured radiance (mw/cm ² sr)				
L_{max}	Max CAL3 radiance (mw/cm ² sr)	3.00	2.00	1.75	4.00
H_n/H	Ratio of irradiance under new conditions to original conditions	1.8	1.8	1.8	1.8
$\frac{\Delta_c(L)}{L}$	Systematic error in LANDSAT MSS absolute calibration	0.15	0.15	0.15	0.15
C	Change in path radiance caused by illumination transformation = $L_{pn} - \frac{H_n}{H} L_p$	0.102	0.046	0.078	0.063
$\Delta_T(C)$	Error in path radiance change due to transmission assumption	-.031	-.019	-.030	-.070
$\Delta_m(C)$	Error in path radiance change due to errors in model	+0.001	-0.009	+0.021	-0.008

Table 8

Systematic Errors in Illumination Transformation for the Four LANDSAT Bands

<u>Radiance Level</u>	<u>Units</u>	<u>Band 4</u>	<u>Band 5</u>	<u>Band 6</u>	<u>Band 7</u>
Low (L = L _p)	Absolute (mw/cm ² sr)*	0.083	0.049	0.055	0.086
High (L = $\frac{1}{2}L_{max}$ ^s)	Absolute (mw/cm ² sr)	0.406	0.271	0.235	0.545
Low (L = L _p)	CAL3 LANDSAT Digital units [†]	2.6	2.7	5.3	4.5
High (L = $\frac{1}{2}L_{max}$)	CAL3 LANDSAT Digital units	2.6	2.7	5.3	4.5

* Systematic error in LANDSAT absolute radiometric calibration included in this calculation.

† Systematic error in LANDSAT absolute radiometric calibration excluded in this calculation.

^s The original radiance was taken at half-scale because the new radiance is 1.8 times the original.

Table 9

Variables Used in Error Analysis for Radiance Transformation
to Standard Conditions for the Four LANDSAT Bands

<u>Symbol</u>	<u>Description</u>	<u>Band 4</u>	<u>Band 5</u>	<u>Band 6</u>	<u>Band 7</u>
ΔL_s	Systematic error in transformed radiance (mw/cm ² sr)	See Table 10			
L	LANDSAT measured radiance (mw/cm ² sr)				
L_{max}	Maximum CAL3 radiance (mw/cm ² sr)	3.00	2.00	1.75	4.00
L_p	Path radiance (mw/cm ² sr)	0.286	0.164	0.153	0.185
$\frac{H_s T_s}{HT}$	Ratio of illumination and transmission under standard conditions to actual conditions	2.16	2.12	2.07	2.07
$\frac{H_s}{H}$	Change in illumination resulting from change in solar elevation from 25° to 50°	1.8	1.8	1.8	1.8
$\Delta_m \left(\frac{T_s}{T} \right)$	Systematic error in atmospheric transmission correction	0.02	0.03	0.03	0.03
$\frac{\Delta_c(L)}{L}$	Systematic error in LANDSAT MSS absolute calibration	0.15	0.15	0.15	0.15
$\Delta_m(L_{ps})$	Error in model calculation of path radiance under standard conditions (mw/cm ² sr)	0.055	0.056	0.021	0.027

Table 10

Systematic Errors in Radiance Transformation to
Standard Conditions for the Four LANDSAT Bands

Absolute Units (mw/cm ² sr)			<u>Band 4</u>	<u>Band 5</u>	<u>Band 6</u>	<u>Band 7</u>
<u>Line No.</u>	<u>Quantity</u>	<u>Radiance Level</u>				
1	Error in absolute radiance	Low (L=L _p)	0.055	0.056	0.021	0.027
2	Error in absolute radiance	High (H= $\frac{1}{2}$ L _{max})	0.400	0.275	0.229	0.573
3	Error in CAL3 radiance (single scene)	Low (L=L _p)	4.7	7.1	3.1	1.7
4	Differential error in CAL3 radiances (two scenes)	Low	0.	0.	0.	0.
5	Typical atmospheric variation.	Low	8.	8.	14.	11.
6	Error in CAL3 radiance (single scene)	High (L= $\frac{1}{2}$ L _{max})	10.2	9.2	6.5	6.5
7	Differential error in CAL3 radiance (two scenes)	High	6.8	6.4	3.8	2.6
8	Typical atmospheric variation	High	22.	20.	20.	19.